Journal of Applied Sciences

ISSN 1812-5654

science alert

ANSInet
an open access publisher
http://ansinet.com

Journal of Applied Sciences 10 (12): 1044-1051, 2010
ISSN 1812-5654

Effect of Fe Doping on Phase Transition of TiO_2 Nanoparticles Synthesized by MOCVD

S.H. Othman, S. Abdul Rashid, T.I. Mohd Ghazi and N. Abdullah
Department of Chemical and Environmental Engineering, Faculty of Engineering,
University Putra Malaysia, 43400 Serdang, Selangor, Malaysia

Abstract: Titanium dioxide (TiO_2) nanoparticles were prepared via Metal Organic Chemical Vapour Deposition (MOCVD) technique at 400 and 700°C. Different amount of iron (Fe) dopant was introduced inside the MOCVD reactor along with the precursor to produce different Fe dopant concentrations of TiO_2 nanoparticles. Transmission Electron Microscope (TEM) results disclosed that increasing the deposition temperature resulted in a significant decrease of the size of TiO_2 nanoparticle samples and a narrower size distribution. X-ray diffraction (XRD) results revealed that TiO_2 nanoparticle sample deposited at 400°C was amorphous while the sample deposited at 700°C was in anatase crystal structure. Fe doping induced phase transition from amorphous to anatase for sample deposited at 400°C and from anatase to rutile for sample deposited at 700°C. Increased concentration of Fe dopant promoted both phase transitions. Meanwhile, TEM and XRD data disclosed that increased concentration of Fe dopant lead to a decrease in size of the nanoparticles produced.

Key words: Titanium dioxide, Fe-doped, nanoparticles, MOCVD, phase transition

INTRODUCTION

The most popular choice of photocatalyst is titanium dioxide (TiO_2) and much of the published work on photocatalysis uses this material. TiO_2 is a promising photocatalyst due to its easy access, low cost, photoactivity, high stability, non-toxicity, hydrophilicity and high refractive index. It can be used for a variety of applications. Recent applications of TiO_2 have involved self-cleaning, anti-bacterial, air purification and water treatment.

TiO_2 exists in different phases such as amorphous, anatase, brookite and rutile. It has been generally accepted that amorphous TiO_2 has no or negligible photocatalytic activity. Crystal structure of TiO_2 is known to exist in a stable phase called rutile and two metastable phases called anatase and brookite. Anatase and brookite are irreversibly transformed into rutile. However, phase equilibrium does not exist for the transformation and therefore, no specific temperature can be assigned to the phase transition. Although the rutile phase has a wide variety of applications primarily in the pigment industry, most work has shown that the anatase phase with a band gap of 3.2 eV is usually preferred because it has proven to be the most active crystal structure that possesses higher levels of photoactivity due to its favourable energy band positions and high surface area (Nishimoto *et al*., 1985). Addition of dopants such as iron (Fe) into the lattice sites of TiO_2 could improve some of its properties for instance it can reduce the bandgap energy of TiO_2 to encourage them to absorb light at higher wavelength for indoor applications (Zhang and Lei, 2008). Other than that, dopants can help to promote the phase transition from anatase to rutile hence reduce the phase transition temperature (Zhang and Lei, 2008; Ghosh *et al*., 2001). It is also proven in this study that addition of Fe dopant can promote the phase transition from amorphous to anatase. It is vital to produce crystalline TiO_2 before they can be used for applications because amorphous TiO_2 is not photocatalytically active. Apart from that, although anatase phase is preferred over rutile phase for applications, it is also widely accepted that mixed phase of TiO_2 results in better photocatalytic activity than just anatase phase alone. It is therefore important to understand the role played by the dopant in the TiO_2 lattice sites.

A glance through the literature reveals that the synthesis of TiO_2 has been widely studied using various approaches such as pulsed laser deposition (Paily *et al*., 2002), diffusion flame reactor (Jang and Kim, 2001), water in oil emulsion (Mori *et al*., 2001), hydrothermal synthesis (Wu *et al*., 1999; Andersson *et al*., 2007) and metal

Corresponding Author: S.H. Othman, Department of Chemical and Environmental Engineering, Faculty of Engineering, University Putra Malaysia, 43400 Serdang, Selangor, Malaysia
Tel: +006 0389466285 Fax: +006 0386567120

organic chemical vapour deposition (MOCVD) (Li *et al*., 2002). Compared with the other methods, MOCVD is a promising technique for catalyst manufacture due to the ease and simplicity of the process. All the traditional steps in catalyst preparation such as drying, reduction, centrifuge, or hydrothermal processing which critically affect catalyst performance can be eliminated. Another advantage of MOCVD technique is that dopants can be easily introduced into the reactor either through a solid source, separated from precursor, or mixed in with the precursor. Thus, it is possible to produce doped TiO_2 via a one step MOCVD process. Furthermore, the control of size distribution is easily accomplished by simply controlling the deposition temperature and the flow rate of the carrier gas.

The aim of this study was specifically to investigate the effect of Fe doping on phase transition in TiO_2 systems. Furthermore, the effect of Fe doping on the size of nanoparticles produced was also studied. In this work, undoped and Fe-doped TiO_2 nanoparticles were produced at 400 and 700°C deposition temperatures with different concentrations of Fe. To the best of our knowledge, very limited research has been published regarding the effect of Fe doping on the TiO_2 phase transition from amorphous to anatase. Only one study has been done to study the effect of Fe on the phase transition from anatase to rutile of Fe-doped TiO_2 produced using MOCVD (Zhang and Lei, 2008). However that particular study only investigated the effect of deposition temperature on the crystal structure of Fe-doped TiO_2 and not the effect of different concentrations of Fe on the crystal structure of Fe-doped TiO_2. This study will hopefully provide a better understanding of the amorphous to anatase and anatase to rutile phase transitions in TiO_2 as well as the role of Fe in the process.

MATERIALS AND METHODS

Synthesis of undoped and Fe-doped TiO_2 nanoparticles: The MOCVD setup consists of stainless steel gas flow lines, mass flow controllers, a bubbler and a quartz tube (52 mm o.d. and 800 mm long) in a split tube furnace as the reactor. The heating zone was 300 mm long. The precursor, titanium (IV) butoxide (TBOT) obtained from Aldrich was used as received. The TBOT precursor was stored in a stainless steel bubbler located on a hot plate and maintained at 175°C. To produce different Fe dopant concentration of TiO_2 nanoparticles, different amount of Fe precursor which was ferrocene (0.005, 0.01, 0.03 and 0.05 g) was mixed directly with 20 mL TBOT precursor inside the bubbler. The quartz tube was purged by nitrogen (400 mL min^{-1}) during the initial heating step towards reaching the desired deposition temperature (400 and 700°C). Once the reaction temperature was achieved, the precursor was introduced into the quartz tube using nitrogen as the carrier gas (400 mL min^{-1}) along with an oxygen feed (100 mL min^{-1}). Undoped and Fe-doped TiO_2 nanoparticles would be thermophoretically deposited inside the quartz tube upon thermal decomposition of the precursor gas. After 3 h of reaction time, the flow of the precursor gas and the flow of the oxygen gas inside the reactor were stopped by switching off the carrier gas and oxygen gas valves. The reactor was allowed to cool to room temperature under 400 mL min^{-1} nitrogen flow. The nanoparticles were then collected from the quartz tube wall using a spatula and kept in a small container.

Characterization method: The morphology of undoped and Fe-doped TiO_2 nanoparticle samples was studied by Transmission Electron Microscope (TEM) using LEO 912AB Energy Filter TEM. The nanoparticle size in terms of diameter was determined from TEM micrographs using the ImageJ software. The error or tolerance in nanoparticle size determination using the software is ±0.005 nm. The nanoparticle size distribution was presented in histograms that were fitted using Gaussian distribution. The phase of the samples were determined by x-ray diffraction (XRD) using Philips X'pert Pro PW3040 with a Cu Kα radiation source (λ= 0.15406 nm) operated at 40 kV and 30 mA. Energy dispersive x-ray (EDX) analysis via LEO 1455 VP SEM was carried out to determine the elemental composition of the samples and to prove the presence of Fe in the TiO_2 crystal structure.

RESULTS AND DISCUSSION

Undoped TiO_2 nanoparticles: Figure 1a and b compare the TEM micrographs of undoped TiO_2 nanoparticle samples deposited at 400 and 700°C. The respective size distribution histograms of the nanoparticles in terms of diameter are also shown. Mean nanoparticle diameter and standard deviations are also included. The micrographs show that the nominal diameter of the nanoparticles were less than 50 nm and that the nanoparticles appeared to be homogeneous and uniform in size. From Fig. 1, it is clear that increasing deposition temperature has a direct effect on the nanoparticle size. The mean nanoparticle diameter decreased from 35.75 to 10.03 nm when the deposition temperature was increased from 400 to 700°C.

The decrease in nanoparticle diameter as the temperature was increased can be attributed to the improvement of nucleation rate and/or suppression of growth (Shi *et al*., 2000). If there is an increment in the nucleation rate, a greater percentage of the precursor

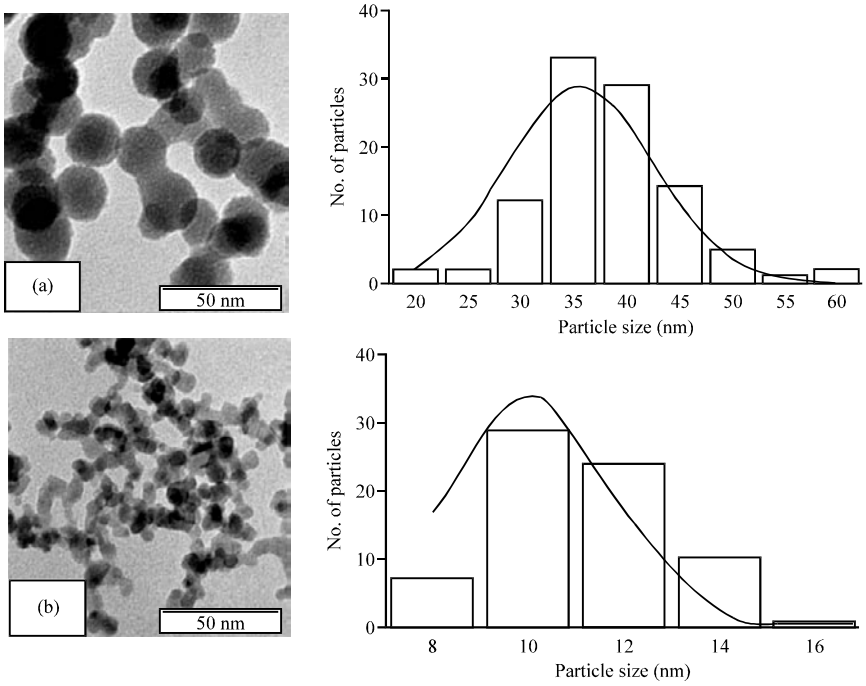

Fig. 1: TEM micrographs (left) and respective nanoparticles size distribution histograms (right) of undoped TiO_2 nanoparticle samples deposited by MOCVD at (a) 400°C and (b) 700°C. The histograms were fitted using Gaussian fittings

vapor can be used to form small particles quickly which would lead to less vapor being available for condensation and further growth (Nolan *et al*., 2006). According to Nakaso *et al*. (2003), at lower reactor temperatures only small amounts of the precursor reacts to form TiO_2. The unreacted precursor condenses out forming partially oxidized Ti that would become TiO_2 upon thermal decomposition (Nakaso *et al*., 2003). This results in large and amorphous particles at lower reaction temperatures. Furthermore, Fig. 1 demonstrates that the increase in temperature causes a decrease in size distribution. This shows that a higher deposition temperature generates smaller nanoparticles with a narrower size distribution.

The crystal structure of undoped TiO_2 nanoparticle samples obtained by XRD is shown in Fig. 2. The XRD pattern for the sample deposited at 400°C showed no detectable peaks, indicating that the sample was amorphous. The peaks at 2θ values of 25.3, 37.8, 48.0, 53.8 and 54.9 for the samples deposited at temperature 700°C correspond to the diffractions of the (1 0 1) (0 0 4) (2 0 0) (1 0 5) (2 1 1) planes of anatase respectively (Li *et al*., 2002; Zhang *et al*., 2006). These peaks confirmed that undoped TiO_2 nanoparticle samples deposited at 700°C were in the anatase phase. From the XRD data, there were no other detectable peaks to suggest the presence of rutile phase.

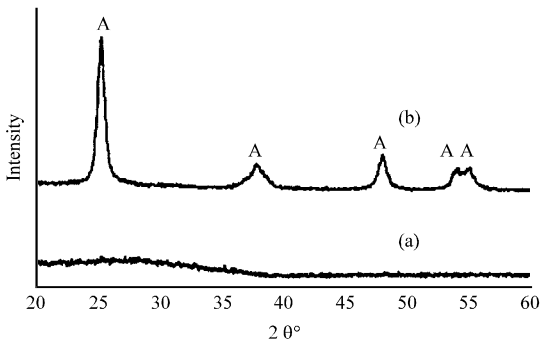

Fig. 2: XRD patterns of undoped TiO_2 nanoparticle samples produced by MOCVD (a) 400°C amorphous and (b) 700°C anatase. A: Anatase

Figure 3a and b compare the EDX spectra of the undoped and Fe-doped TiO_2 nanoparticles (0.03 g Fe). Peaks around 0.4, 4.5 and 5.0 keV correspond to TiO_2 in the sample. The peaks due to iron are clearly distinct in Fe-doped TiO_2 (Fig. 3b) at around 0.7, 6.4 and 7.0 keV thus proving the presence of Fe in the crystal structure of TiO_2. Apart from emission peaks of Ti, O and Fe, the peaks of C and Au were also observed most probably due to the carbon in the TBOT precursor and from the gold coating during sample preparation for EDX analysis, respectively.

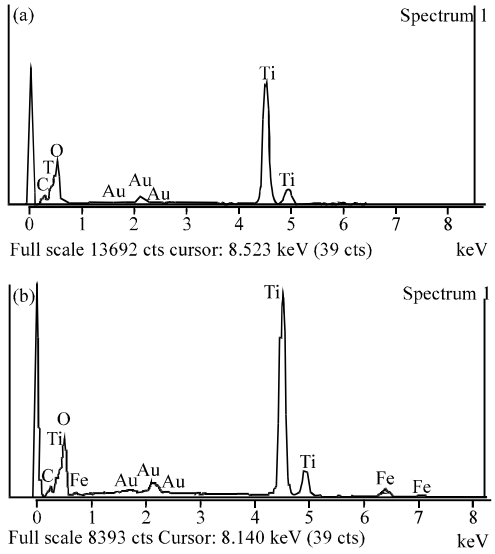

Fig. 3: EDX spectra of undoped and Fe-doped TiO_2 (0.03 g Fe) nanoparticle samples produced by MOCVD at 700°C

Table 1: Effect of amount of Fe dopant on the percentage of anatase and rutile crystal structure and average nanoparticle size of sample deposited at 700°C

Amount of Fe dopant (g)	[a]Fe/Ti ratio	[b]Anatase (%)	[b]Rutile (%)	[c]Average nanoparticle diameter (nm)
0	0	100.0	-	20.7
0.005	0.0041	92.9	7.1	25.6
0.010	0.0107	92.5	7.5	24.8
0.030	0.0667	88.5	11.5	24.6
0.050	0.1317	88.4	11.6	22.5

[a]Determined using EDX, [b]Calculated using Eq. 1, [c]Calculated using Eq. 4

The elemental composition of the samples was also determined via EDX analysis. Fe/Ti ratio (at. %) values are tabulated in Table 1. As expected, it can be seen that Fe/Ti ratio increased with increasing amount of Fe dopant.

Figure 4a-d compare the TEM micrographs of Fe-doped TiO_2 nanoparticle samples deposited at 400 and 700°C with different Fe dopant concentrations. The respective size distribution histograms of the nanoparticles in terms of diameter are also shown. The micrographs show that the nominal diameter of the nanoparticles was still less than 50 nm and that the nanoparticles appeared to be homogeneous and uniform in size. From Fig. 4, it can be seen that the effect of deposition temperature on nanoparticle size of Fe-doped TiO_2 samples is similar to undoped samples. Furthermore, Fig. 4 also shows that the nanoparticle diameter of samples deposited at a certain temperature is about the same no matter how much Fe dopant was introduced. However, the histograms demonstrated that the mean nanoparticle diameter decreased with an increase of the Fe dopant concentration. This is probably due to the fact that Fe doping slowers the growth of the TiO_2 (Naeem and Ouyang, 2010). This finding is also supported by Zhou *et al.* (2005). Nonetheless, the difference is relatively small.

The crystal structure of undoped and Fe-doped TiO_2 nanoparticle samples obtained by XRD are shown in Fig. 5. No characteristic peaks of iron oxide phases appeared in the XRD spectra for all the samples. This was probably attributed to the fact that the Fe dopant concentration was very low and hence could not be detected by XRD.

From Fig. 5a, the XRD pattern for the undoped sample deposited at 400°C showed no detectable peaks indicating that the sample was amorphous. However, as the Fe dopant concentration was increased, the peaks at 2θ values of 25.3, 37.8, 48.0, 53.8 and 54.9 started to appear which correspond to the diffractions of the (1 0 1) (0 0 4) (2 0 0) (1 0 5) (2 1 1) planes of anatase respectively (Li *et al.*, 2002; Zhang *et al.*, 2006). It is known that from the effective radius of ions for a coordination number of 6, Fe^{3+} has an ionic radius (0.645Å) comparable to Ti^{4+} (0.605 Å) (Shannon, 1976). Therefore, Fe^{3+} can easily substitute Ti^{4+} in the TiO_2 lattice sites and distort the crystal structure of the host compound. The oxidation state of Fe in the samples is currently unknown but can be determined from x-ray photoelectron spectroscopy (XPS). However, the transition from amorphous to anatase crystal structure as can be seen from Fig. 5a seems to suggest that Fe dopant does indeed induce crystallization. This finding is consistent with the finding of Zhang and Reller (2002) who used sol-gel technique to prepare homogeneously doped TiO_2. Their study demonstrated that Fe doping could cause phase transition from amorphous to anatase at lower calcination temperature. Furthermore, the peak intensity corresponding to the anatase crystal structure increased as the Fe concentration was increased. This indicated that increasing the Fe dopant concentration can promote the formation of anatase phase. Naeem and Ouyang (2010) established the same trend of results for lower Fe dopant concentrations.

Figure 5b shows that undoped samples deposited at 700°C were in the anatase phase. Nonetheless, as the Fe dopant was introduced into the TiO_2 lattice, new apparent peaks started to appear. These new peaks at 2θ values of 27.4, 36.1 and 41.23 corresponds to the diffractions of the (1 1 0) (1 0 1) and (1 1 1) planes of rutile, respectively (Jitputti *et al.*, 2007). These peaks indicated that the sample had a mixture of anatase and rutile crystal structure. The fractions of anatase and rutile crystal structure were calculated according to the following equation (Yan *et al.*, 2005):

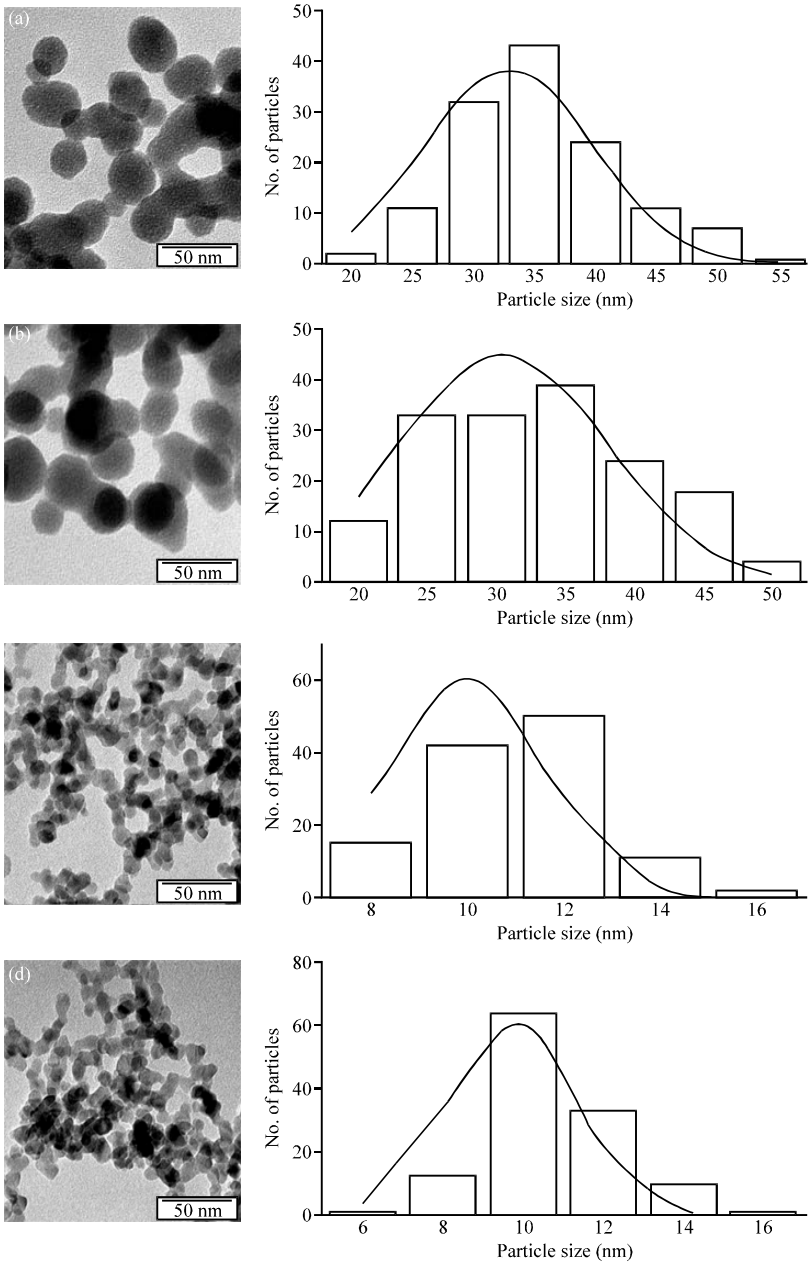

Fig. 4: TEM micrographs (left) and respective nanoparticles size distribution histograms (right) of TiO_2 nanoparticle samples deposited by MOCVD at (a) 400°C-0.01 g Fe dopant, Mean = 32.92 nm, STD = 6.84 (b) 400°C-0.05 g Fe dopant, Mean = 30.53 nm, STD = 7.56 (c) 700°C-0.01 g Fe dopant, Mean = 9.98 nm, STD = 1.63 and (d) 700°C -0.05 g Fe dopant, Mean = 9.71 nm, STD = 1.58. The histograms were fitted using Gaussian fittings

$$f_A = \frac{1}{1 + \frac{1}{K}\frac{I_R}{I_A}}$$
$$K = 0.79 \quad f_A > 0.2$$
$$K = 0.68 \quad f_A \leq 0.2 \qquad (1)$$

where, f_A is the fraction of anatase crystal structure in the samples, I_A and I_R are the X-ray intensities of the anatase (1 0 1) and rutile (1 1 0) diffraction peaks, respectively and K is a constant. The percentage of anatase and rutile crystal structure was tabulated in Table 1.

Table 1 illustrates that the percentage of rutile increases with the increase in Fe dopant concentration. This finding is supported by Fig. 5b where there seems to be a decrease in the peak intensity for (1 0 1) plane of anatase as the amount of Fe dopant increases. A decrease

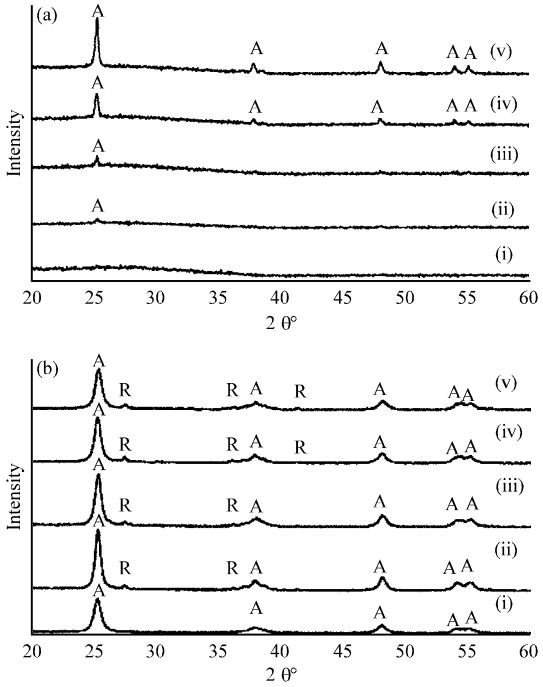

Fig. 5: XRD patterns of undoped and Fe-doped TiO_2 nanoparticle samples produced by MOCVD (a) 400°C and (b) 700°C. A: Anatase, R: Rutile

of the anatase phase with the increase of the Fe dopant concentration compensates the increase of rutile fraction (Alexandrescu *et al*., 2007). Hence it is concluded that Fe doping into the TiO_2 lattice can promote the anatase to rutile phase transition. Although the oxidation state for Fe in the samples are unknown, it is speculated that considering the ionic radius of Ti^{4+} and Fe^{3+} is almost the same, Fe^{3+} could replace the Ti^{4+} in lattice sites and therefore forming a solid solution of Fe in the TiO_2 matrix. Consequently, this causes oxygen vacancies because of charge compensation and their movement would favor the rutile nucleation in anatase particles (Zhang and Lei, 2008). Further characterization of the samples using XPS would be able to support the findings.

Note that the anatase to rutile transition is a metastable to stable transformation. However, it is generally accepted that phase equilibrium does not exist for the anatase to rutile transformation and therefore, no specific temperature can be assigned to the phase transition. The Gibbs free energy for the two phases is as follows (Liao *et al*., 1997):

$$G_{anatase}\,(J/mol) = -966798.3 + 463.4075T + \frac{0.854\times10^{6}}{T} + 0.312\times10^{-6}T^{3} + 0.763\sqrt{T} - 75.323T\ln T + 1.124\times10^{-3}T^{2} \quad (2)$$

$$G_{rutile}\,(J/mol) = -969145.6 + 462.5506T + \frac{0.711\times10^{6}}{T} + 0.202\times10^{-6}T^{3} - 304.762\sqrt{T} - 73.799T\ln T - 3.014\times10^{-3}T^{2} \quad (3)$$

where, G is the Gibbs free energy and T is the temperature. The energy difference, ÄG between the anatase and the rutile phases at 700°C is 6674.56 J/mol, which is the driving force for rutile nucleation.

Shannon and Pask (1965) hypothesized that oxygen vacancies reduces the energy that must be overcome before the rearrangement of the Ti-O octahedra can occur to cause phase transition from anatase to rutile. Thus, it is speculated that the mechanism responsible to promote the phase transition from anatase to rutile is the oxygen vacancies due to Fe doping. Gosh *et al*. (2001) also reported that the addition of Fe could promote the transition of anatase to rutile.

Moreover, Fig. 5b shows that Fe doping has a direct albeit small effect on the size of the Fe-doped TiO_2 nanoparticles. It can be seen from Fig. 5b that the greater the concentration of Fe, the wider the width of anatase (1 0 1) diffraction peak and therefore the smaller the grain size of Fe-doped TiO_2 nanoparticles. The mean nanoparticle diameter of the samples was calculated by applying the Debye-Scherrer formula (Yan *et al*., 2005) on the anatase (1 0 1) diffraction peaks;

$$D = \frac{K\lambda}{\beta\cos\theta} \quad (4)$$

where, D is the mean nanoparticle diameter, K is a constant which is taken as 0.89 for spherical crystalline shape, λ is the wavelength of the X-ray radiation (Cu Kα = 0.15406 nm), β is the corrected band broadening at full width at half-maximum (fwhm) and θ is the diffraction angle.

The results are also tabulated in Table 1. The results demonstrate that the mean nanoparticle diameter decreased with an increase of the Fe dopant concentration although the difference is very small (≈2 nm). This finding seems to support the TEM results that were discussed earlier. Regardless of the deviation in the values calculated using Debye Scherrer formula, the results are consistent with the values obtained from the TEM micrographs. Note that the Debye-Scherrer formula is not accurate at estimating nanoparticles size because the assumption of an underlying crystal structure (translational symmetry) is often invalid (Hall *et al*., 2000).

CONCLUSION

In this study, undoped and Fe-doped TiO_2 nanoparticles were successfully synthesized via a one

step MOCVD method at 400 and 700°C deposition temperatures. Major effects of Fe doping found in this study are: 1) promote the phase transition from amorphous to anatase and from anatase to rutile 2) nanoparticle size decreases with an increase in Fe dopant concentration. TEM results disclosed that in general, the average nanoparticle size decreases with increasing temperature. XRD data revealed that the undoped TiO_2 nanoparticle sample deposited at 400°C was amorphous but the addition of Fe dopant induces crystallization of the sample. Increasing the amount of Fe dopant promoted the phase transition from amorphous to anatase phase. Meanwhile, the undoped TiO_2 nanoparticle sample deposited at 700°C was in anatase crystal structure. Fe doping causes phase transition from anatase to rutile crystal structure. Increasing the amount of Fe dopant reduces the mean nanoparticle size and reduces the anatase fraction. Fe doping also promoted the phase transition from anatase to rutile due to the oxygen vacancies in TiO_2 lattice sites.

ACKNOWLEDGMENTS

This study was financially supported by Fundamental Research Grant Scheme, University Putra Malaysia (Grant No. 5523426).

REFERENCES

Alexandrescu, R., I. Morjan, M. Scarisoreanu, R. Birjega and E. Popovici *et al*., 2007. Structural investigations of TiO_2 and Fe-doped TiO_2 nanoparticles synthesized by laser pyrolysis. Thin Solid Films, 515: 8438-8445.

Andersson, M., A. Kiselev, L. Osterlund and A.E.C. Palmqvist, 2007. Microemulsion-mediated room-temperature synthesis of high-surface-area rutile and its photocatalytic performance. J. Phys. Chem. C, 111: 6789-6797.

Ghosh, S.K., A.K. Vasudevan, P.P. Rao and K.G.K. Warrier, 2001. Influence of different additives on anatase–rutile transformation in titania system. Br. Ceramic Trans., 100: 151-154.

Hall, B.D., D. Zanchet and D. Ugarte, 2000. Estimating nanoparticle size from diffraction measurements. J. Applied Crystallography, 33: 1335-1341.

Jang, H.D. and S.K. Kim, 2001. Controlled synthesis of titanium dioxide nanoparticles in a modified diffusion flame reactor. Mater. Res. Bull., 36: 627-637.

Jitputti, J., S. Pavasupreea, Y. Suzukia and S. Yoshikawaa, 2007. Synthesis and photocatalytic activity for water-splitting reaction of nanocrystalline mesoporous titania prepared by hydrothermal method. J. Solid State Chem., 180: 1743-1749.

Li, W., S.I. Shah, C.P. Huang, O. Jung and C. Ni, 2002. Metallorganic chemical vapor deposition and characterization of TiO_2 nanoparticles. Mater. Sci. Eng. B, 96: 247-253.

Liao, S.C., W.E. Mayo and K.D. Pae, 1997. Theory of high pressure/low temperature sintering of bulk nanocrystalline TiO_2. Acta Mater., 45: 4027-4040.

Mori, Y., Y. Okastu and Y. Tsujimoto, 2001. Titanium dioxide nanoparticles produced in water-in-oil emulsion. J. Nanopartical Res., 3: 219-225.

Naeem, K. and F. Ouyang, 2010. Preparation of Fe3+-doped TiO_2 nanoparticles and its photocatalytic activity under UV light. Phys. B: Condensed Matter, 405: 221-226.

Nakaso, K., K. Okuyama, M. Shimada and S.E. Pratsinis, 2003. Effect of reaction temperature on CVD-made TiO_2 primary particle diameter. Chem. Eng. Sci., 58: 3327-3335.

Nishimoto, S., B. Ohtani, H. Kajiwara and T. Kagiya, 1985. Correlation of the crystal structure of titanium dioxide prepared from titanium tetra-2-propoxide with the photocatalytic activity for redox reactions in aqueous propan-2-ol and silver salt solutions. J. Chem. Soc., 81: 61-68.

Nolan, M.G., M.E. Pemble, D.W. Sheel and H.M. Yates, 2006. One step process for chemical vapour deposition of titanium dioxide thin films incorporating controlled structure nanoparticles. Thin Solid Films, 515: 1956-1962.

Paily, R., A. DasGasputa, N. DasGasputa, P. Bhattacharya and P. Mista *et al*., 2002. Pulsed laser deposition of TiO_2 for MOS gate dielectric. Applied Surface Sci., 187: 297-304.

Shannon, R.D. and J.A. Pask, 1965. Kinetics of the anatase-rutile transformation. J. Am. Ceramic Soc., 48: 391-398.

Shannon, R.D., 1976. Revised effective ionic radii and systematic studies of interatomic distances in halides and chalcogenides. Acta Crystallography, 32: 751-767.

Shi, L., C. Li, A. Chen, A. Zhu, Z. Yihua and D. Fang, 2000. Morphology and structure of nanosized TiO_2 particles synthesized by gas-phase reaction. Mater. Chem. Phys., 66: 51-57.

Wu, M., J. Long, A. Huang and Y. Luo, 1999. Microemulsion-mediated hydrothermal synthesis and characterization of nanosize rutile and anatase particles. Langmuir, 15: 8822-8825.

Yan, M., F. Chen, J. Zhang and M. Anpo, 2005. Preparation of controllable crystalline titania and study on the photocatalytic properties. J. Phys. Chem. B, 109: 8673-8678.

Zhang, Y.H. and A. Reller, 2002. Phase transformation and grain growth of doped nanosized titania. Mater. Sci. Eng. C, 19: 323-326.

Zhang, X.W., M.H. Zhou and L.C. Lei, 2006. Co-deposition of photocatalytic Fe doped TiO_2 coatings by MOCVD. Catalysis Commun., 7: 427-431.

Zhang, X. and L. Lei, 2008. One step preparation of visible-light responsive Fe-TiO_2 coating photocatalysts by MOCVD. Mater. Lett., 62: 895-897.

Zhou, M., J. Yu, B. Cheng and H. Yu, 2005. Preparation and photocatalytic activity of Fe-doped mesoporous titanium dioxide nanocrystalline photocatalysts. Mater. Chem. Phys., 93: 159-163.